

A CONSISTENT MATHEMATICAL MODEL TO SIMULATE
STEADY AND UNSTEADY ROTOR-BLADE AERODYNAMICS

BY

U. LEISS

UNIVERSITY OF THE FEDERAL

ARMED FORCES MUNICH

TENTH EUROPEAN ROTORCRAFT FORUM
AUGUST 28 – 31, 1984 – THE HAGUE, THE NETHERLANDS

A CONSISTENT MATHEMATICAL MODEL TO SIMULATE STEADY AND UNSTEADY ROTOR-BLADE AERODYNAMICS



BY

U. LEISS

UNIVERSITY OF THE FEDERAL
ARMED FORCES MUNICH

ABSTRACT: A general formulation has been developed to simulate the stalled and unstalled aerodynamic coefficients of a rotor blade in steady and unsteady flow. The main features of the present method are few empirical parameters with physical background in the full range in angle of attack and Mach number without the need to sectionize the validity of parameters. The method takes account for different types of steady stall and the influence of Reynolds number. Unsteady effects due to pitch, plunge and fore and aft motion are separately implemented. The calculated steady normal force coefficient curve and the unsteady hysteresis loops of the present method match very well with the twodimensional test data, even for high frequencies. In addition some comparisons with other methods are presented. Aerodynamic rotor forces can be obtained by analytical integration of the section forces over the span of the blade and analytical derivatives of these forces are possible.

NOTATION

a	speed of sound	<u>Subscripts</u>	
Amp	amplitude	AC	aerodynamic center
b_i	approximation coefficients	ai	aircraft induced
c	airfoil chord	b	bubble
c_i	coefficients (empirical)	bb	bubble burst
cr	airfoil camber (z/c)	c	curvature
f	oscillation frequency	e	extremal
k	reduced frequency	fa	free air
M	Mach number	i	numbering index
q_a	dynamic sonic pressure	k	Küssner
Re	Reynolds number	m	magnitude
t	airfoil thickness (z/c)	nc	noncirculatory
v	velocity	os	overshoot
x,y,z	rotor blade fixed coordinates	ref	reference condition
β_i	approximation coefficients	spc	supercritical
ρ	air density	ss	static stall
ν	kinematical viscosity	vp	vortex proximity
ω	rotor rotational frequency	w	Wagner
φ	phase angle	x,y,z	coordinate direction
		+,-	positive or negative circulation
	circulation	<u>Definitions</u>	
	dimensionless circulation	.	= d/dt
		..	= d ² /dt ²

INTRODUCTION

To calculate the aerodynamic loads of a helicopter rotor usually the twodimensional steady aerodynamic characteristics of the airfoil are used in tabular form or by curve fitting of certain complicated polynomials. In recent years the unsteady models, (Refs. 1-3) based on the steady characteristics, indicated a significant progress, but a lot of empirical parameters and numerical treatment are still necessary. The limitations of these methods and the need of a general easy to use model have led to a new consistent formulation of nonlinear steady and unsteady rotor blade aerodynamics.

The first step was a continuous analytical representation for the steady case of attached flow, partially stalled flow and fully separated flow by a superposition principle. New mission requirements of a helicopter like supermaneuverability must be covered by mathematical rotor models. Extremely high angles of attack and low supersonic flow conditions could occur at certain flight maneuvers. Empirical parameters with a physical background describe in the present method stall and compressibility effects.

On this steady basis the three existing unsteady types of motion were formulated with only few parameters. The most difficult design point of the method was the analytic integrability in radial direction of the rotor blade to avoid numerical problems and to be the basis of more convergent optimization analyses.

If somebody desires much more accuracy for any special case it is possible to refine this modular method without a change of the basic structure.

DEFINITIONS

The orientation of any arbitrary 2-D rotor blade section is defined by the following airfoil fixed cartesian coordinates. The x axis is identical with the chordline and the origin of the system is the elastic axis EA as shown in fig. 1

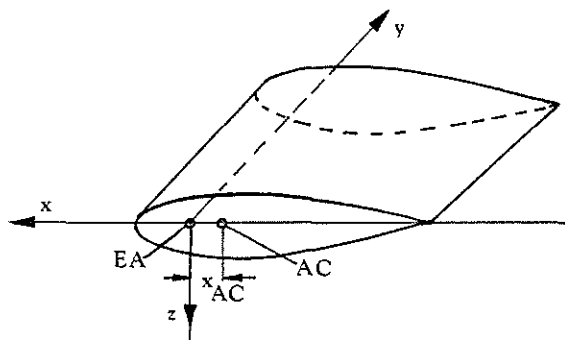


Fig.1 Profile fixed coordinate system

The time derivation of the coordinates gives the velocities \dot{x} , \dot{y} , \dot{z} and accelerations \ddot{x} , \ddot{y} , \ddot{z} . The

only rotational degree of freedom α about the y axis is equivalent to $dz/dx \cdot x$, the angular velocity is $\dot{\alpha}$ or $d\alpha/dx \cdot x$ and the acceleration $\ddot{\alpha}$ or $d^2\alpha/dx^2 \cdot x$. Fig. 2 shows the three types of motion and their corresponding velocity distributions.

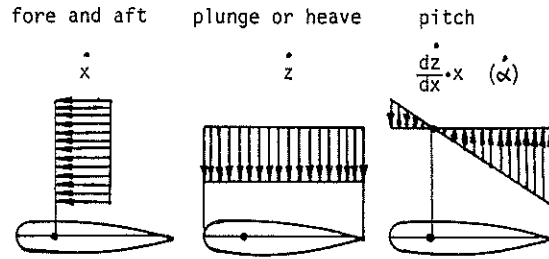


Fig.2 Velocity distribution for different kinds of motion

Plunge and fore and aft motion are blade fixed for a clear definition. The classical resultant velocity fixed definition of Theodorsen (Ref. 4) makes only sense for the small angle assumption $\cos\alpha = 1$ and $\sin\alpha = \alpha$. Because at 90° angle of attack fore and aft motion would be the same like plunge motion at 0° angle of attack and vice versa, the definition is not consistent with the physical effect. It is a common practice to write the aerodynamic forces in the form:

$$d F_{aero} = \frac{\rho}{2} v_{res}^2 \cdot c_{aero}(\alpha, M) \cdot c \cdot dy \quad (1)$$

For a fixed wing aircraft the dynamic pressure is constant, on the other hand at a helicopter rotor blade the dynamic pressure varies significantly in radial direction. Consequently the new definition for the whole helicopter is the dynamic sonic pressure:

$$q_a = \frac{\rho}{2} \cdot a^2 \quad (2)$$

with q_a rewrite eq. 1 as follows:

$$d F_{aero} = q_a \cdot c_{aero}(\alpha, M) \cdot M^2 \cdot c \cdot dy \quad (3)$$

Here the angle of attack and resultant Mach number dependent coefficient c_{aero} multiplied by the square of Mach number is new defined in the following form:

$$c_{aero}(\alpha, M) \cdot M^2 \longrightarrow c_{x,z}(M_x, M_z) \quad (4)$$

were

$$M_x = \frac{1}{a} (v_{x_{ai}} + v_{x_{fa}} - \dot{x}) \quad (5)$$

$$M_z = \frac{1}{a} (v_{z_{ai}} + v_{z_{fa}} - \dot{z}) \quad (6)$$

The compressible aerodynamic flow condition is indicated by the Mach number components consisting of velocity components induced by the aircraft $v_{x,z_{ai}}$, due to free air motion $v_{x,z_{fa}}$ and blade element motion x, z relative to quiet air. In this general form the formulation can be coupled with the local velocities of any wake and gust model.

Fig. 3 shows the qualitative data range of the α, M dependent aerodynamic coefficients in comparison to the same data range of the compact Mach number component formulation of fig. 4.

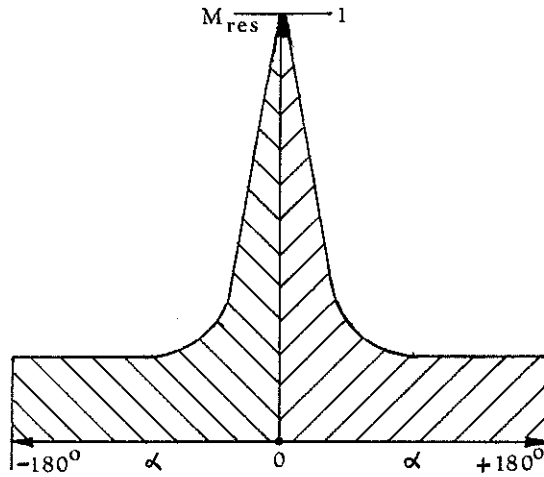


Fig.3 Data range in classical polar coordinates

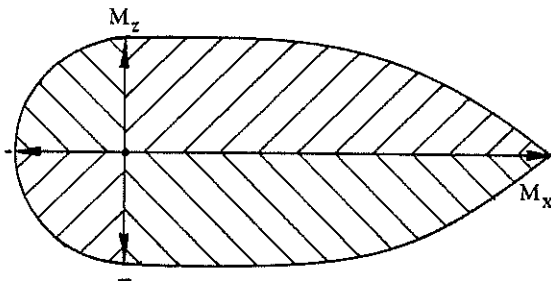


Fig.4 Data range in cartesian coordinates

STEADY 2-D AERODYNAMIC COEFFICIENTS

In the following the formulation of the aerodynamic coefficients is presented for the normal force. The structure for the chordwise force and for the moment is similar.

FULLY SEPARATED FLOW

The normal force coefficient in the fully separated flow condition of an airfoil corresponding to Hoerner (Ref. 5), Critzos (Ref. 6) and some data in the helicopter DATCOM (Ref. 7) can be written for a flat plate:

$$c_z = 2 \cdot M_z \cdot \sqrt{M_x^2 + M_z^2} \quad (7)$$

Considering the influence of thickness and camber leads to:

$$c_z = (2 - f(t)) \cdot M_z \cdot \sqrt{M_x^2 + M_z^2} + f(cr) \cdot M_z^2 \quad (8)$$

Eq. (8) is approximately not limited in M_x or M_z .

INCOMPRESSIBLE ATTACHED FLOW AND TYPES OF STALL

The simple linear aerodynamic theory for attached flow is only valid up to the static stall angle or some degrees below which depends on the type of stall. For helicopter application it is necessary to formulate the boundary layer influence respectively more or less the gradual separation effect. It is a basic assumption that the attached flow region consists of the previous presented fully separated terms and of an additional circulatory function which shows Fig. 5.

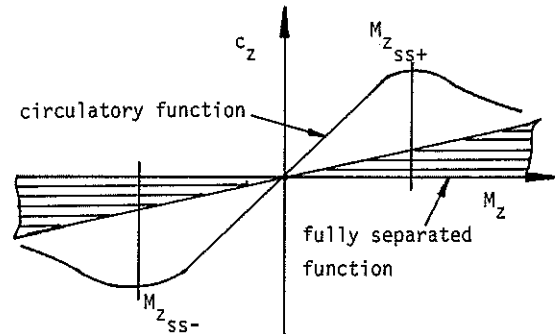


Fig. 5 Superposition of terms for attached flow

For a gradual thin airfoil- or trailing edge stall the dimensionless circulation can be written analytically as given below:

$$\bar{c}_z = \frac{\bar{c}_z^+ + \bar{c}_z^-}{a \cdot c} \quad (9)$$

$$\bar{c}_z^+ = \frac{M_{z_{ss+}}^3 \cdot c_{ss+}}{(M_z - M_{z_{ss+}})^2 + M_{z_{ss+}} \cdot c_{ss+}} \cdot \frac{dc_{z_{ss+}}}{dM_z} \quad (10)$$

$$\bar{c}_z^- = \frac{M_{z_{ss-}}^3 \cdot c_{ss-}}{(M_z - M_{z_{ss-}})^2 + M_{z_{ss-}} \cdot c_{ss-}} \cdot \frac{dc_{z_{ss-}}}{dM_z} \quad (11)$$

The maximum circulation point $M_{z_{ss}}$, the circulation function curvature c_{ss} and $\frac{dc_{z_{ss}}}{dM_z}$ the derivative of the circulation magnitude $dc_{z_{ss}}/dM_z$ describe the positive and negative circulation function.

Though the negative stall region is more of academic nature it should be included for a general representation of any arbitrary nonsymmetric airfoil section. Indeed the present formulation describes the linear behavior within the positive and negative stall points as well as the gradual loss of circulation and the continuous transition to the fully separated flow.

There exists one additional flow phenomenon, the so called leading edge stall which is not covered by the previous circulation function because of its abrupt nature. A short bubble on the airfoil rounds the shape and delays the separation but at sufficient high angles of attack the bubble suddenly bursts and the airfoil stalls totally. This mechanism can be simulated by the following expression for positive or negative leading edge stall:

$$\overline{c}_{b+,-} = \frac{(M_{z_{bb+,-}} - M_z) \cdot M_{z_{be+,-}}^2}{(M_{z_{bb+,-}} - M_z)^2 + M_{z_{be+,-}}^2} \cdot c_{b+,-} \quad (12)$$

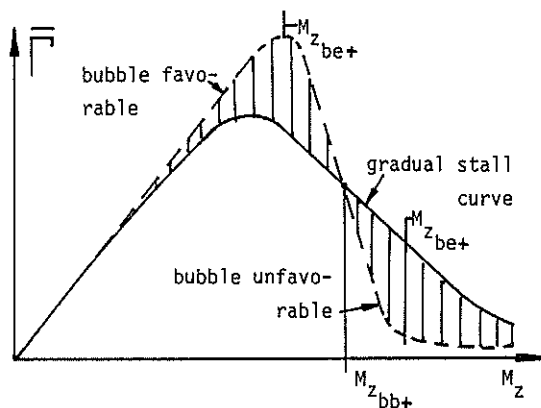


Fig. 6 Influence of the short bubble on leading edge stall

Fig. 6 shows this function and its application on the gradual circulation curve. Now all three types of stall can be simulated by the above two expressions.

INFLUENCE OF REYNOLDS NUMBER

The occurrence of the different types of stall depends on the Reynolds number as shown for a typical case in Ref. 7. For consistence in the present method the Reynolds number is redefined as follows:

$$Re = \frac{a \cdot M_x \cdot c}{\nu} \quad (13)$$

Based on Wayne Johnsons extensive study (Ref. 8) on Reynolds number trends here is assumed the following linear law:

$$\Delta M_{z_{ss+,-}}, \Delta M_{z_{bb+,-}} = c_{Re} \cdot \left(\frac{Re}{Re_{ref}} - 1 \right) \quad (14)$$

were for a fixed Mach number M_x

$$\frac{Re}{Re_{ref}} = \frac{a \cdot c \cdot \nu_{ref}}{\nu \cdot a_{ref} \cdot c_{ref}} \quad (15)$$

The Reynolds number variation results in a movement of the stall point and the bubble burst point as mentioned in Eq. (14).

The coefficient c_{b+} of Eq. (12) extended for the influence of Reynolds number leads to:

$$c_{b+,-} = c_{b+,-} \frac{c_{bRe}}{(Re - Re_{be})^2 + c_{bRe}} \quad (16)$$

Eq. (16) connects the growths of the bubble with Reynolds number. By the expressions of Eq. (15) and (16) the effect of Reynolds number is essential due to chord length variation because the Mach number is fixed and the kinematical viscosity ν varies not greatly.

COMPRESSIBILITY EFFECTS

For inclusion of compressibility effects in the earlier mentioned circulation function two parameters of Eq. (10) or (11) are highly appropriate to be a function of the Mach number component M_x .

The first one is the maximum circulation point $M_{z_{ss}}$. Fig. 7 shows some Mach number dependent measurement results for different airfoils.

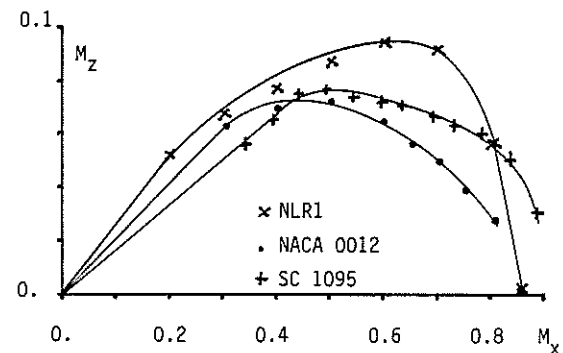


Fig. 7 Stall boundary for different airfoils (Ref. 7)

The typical behavior is similar for all airfoils and represents the transition boundary from sub-critical to supercritical flow conditions. Here the physical effect is expressed by the second order polynomial:

$$M_{z_{ss}} = M_x \cdot (c_1 + c_2 \cdot M_x + c_3 \cdot M_x^2) \quad (17)$$

The coefficients $c_{1,2,3}$ describe the position of the stall point at incompressible conditions, compressibility onset and high subsonic Mach numbers.

The other important parameter, the derivative $dc_{z_{ss}}/dM_x$ is similar to the well known lift curve slope. The Prandtl-Glauert compressibility rule can be applied so far the local Mach number 1 on the airfoil surface is not reached. In the real physics a significant flow change by a shock wave is often delayed up to a local Mach number of about 1.2. If supercritical flow is over a substantial portion of the airfoil surface, the here defined circulation function must vanish.

Hence it is necessary to introduce a new flow function for supercritical flow and to combine with the circulation function because in the transition region subcritical and supercritical flow coexist.

The subsonic lift curve slope theory of Prandtl Glauert and the supersonic one of Ackeret are valid outside of transonic flow conditions. The real shape in the transonic range, presented by Ref. 9 looks different for thick and thin airfoils as indicated in Fig. 8.

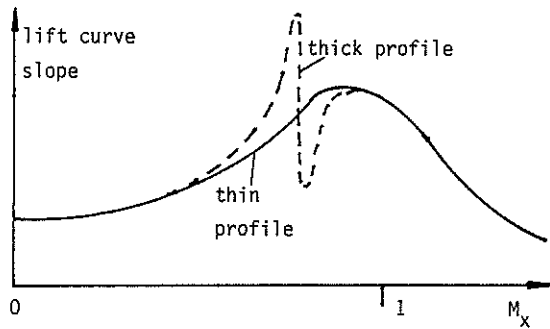


Fig. 8 Typical compressible lift curve slope trends

The reason for this difference is on the one side a supercritical flow field which is nearly independent of the airfoil shape and on the other side the superposition of the greatly on the airfoil shape varying circulation function. (Eq. (10),(11),(17)). The easiest expression for the supercritical flow function is:

$$c_{z_{spc}} = \frac{M_z \cdot M_x^2 \cdot c_{spcm}}{(\sqrt{M_x^2 + M_z^2} - c_{spce})^2 + c_{spcc}} \quad (18)$$

The parameter c_{spce} is the maximum of the function close to sonic speed, c_{spcc} is the curvature and c_{spcm} the magnitude of the function. The representation of a thick and thin airfoil leads back to the unknown derivative $dc_{z_{ss}}/dM_x$ which must be the difference between the z_{ss} resultant curves of Fig. 8 and Eq. (18). The requirements for a Mach number dependent derivative function are a positive and negative peak for the thick airfoil or a positive peak and sharp decrease to zero for the thin airfoil. The formulation of these physical effects can be written in terms of M_x :

$$\frac{dc_{z_{ss}}}{dM_x} = \frac{c_4 \cdot c_5}{M_x^2 + c_5} + \frac{c_6 \cdot (c_7 - M_x)}{(c_8 - M_x)^2 + c_9} \quad (19)$$

The parameter c_4 is the incompressible amount of the derivative, c_5 represents the curvature. The other term evaluates the peaks by the coefficients $c_{6,7,8,9}$.

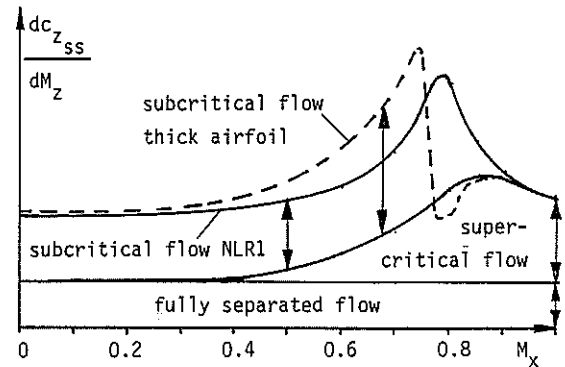


Fig. 9 Flow functions for compressibility effects

Fig. 9 shows the simulation of both airfoils. The thin airfoil has only one maximum due to high subcritical flow Mach numbers and hence the coincidence of the maxima of Eq. (18) and Eq. (19). For a thick airfoil the lift breaks down at relative low Mach numbers so the supercritical flow has a maximum again.

COMPARISON OF THE STEADY SIMULATION MODEL WITH TEST DATA

The compared test data were generated at Boeing Vertol by Dadone (Ref. 10). The NLR1 airfoil was measured in a Mach number range from 0.2 to 0.9 with some blockage effects at high Mach numbers and angles of attack. The parameters of a basic version of the present steady aerodynamic simulation method were obtained by a nonlinear least

square method. The excellent correlation between the non smoothed test data and the mathematical model as illustrated by Fig. 10 demonstrates the generality of the method for all flow conditions.

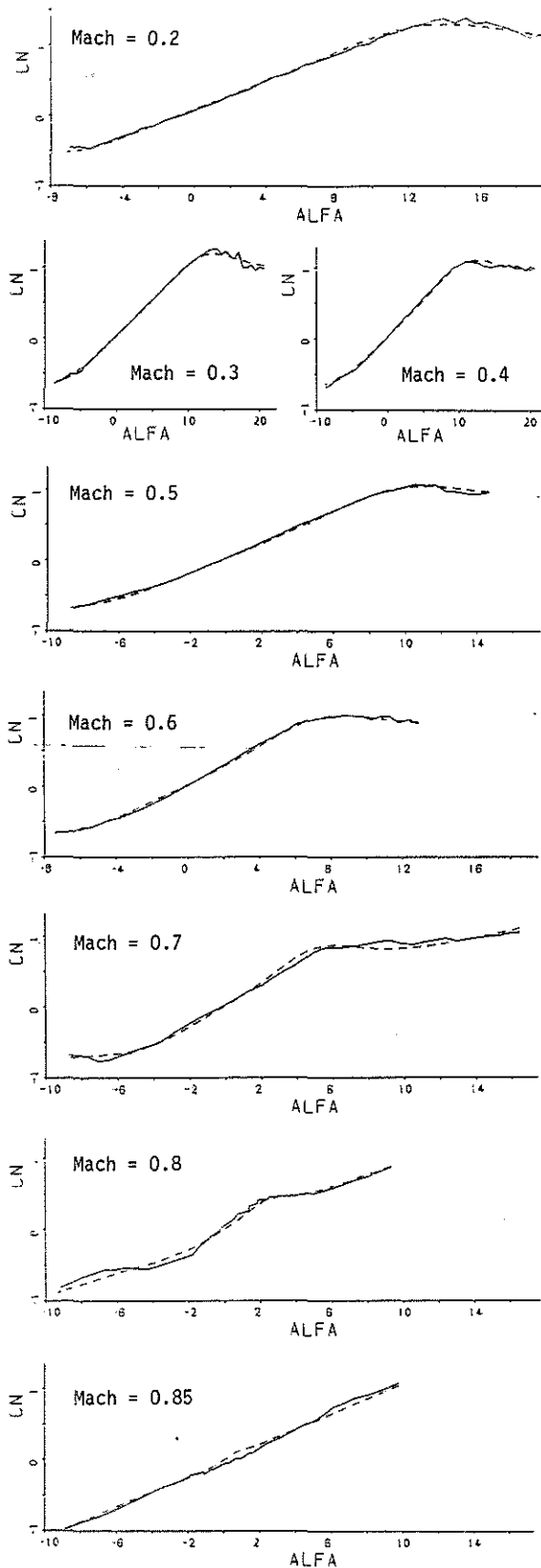


Fig. 10 Comparison of NLR1 data with theory
 — test - - - theory

The mean square root error of the normal force coefficient c_n at 399 data points was lower than 0.05.

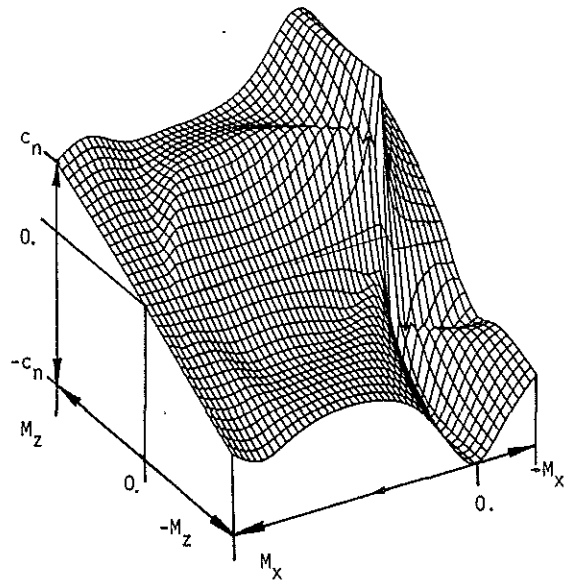


Fig.11 Normal force coefficient versus Mach number components

In Fig. 11 the normal force coefficient is shown including the fully separated and reverse flow.

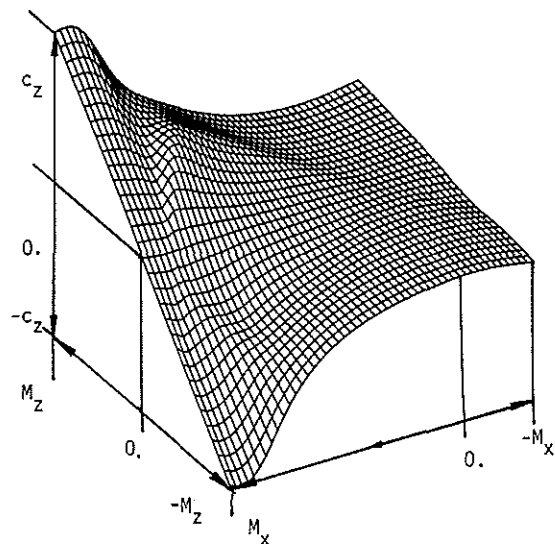


Fig. 12 New normal force coefficient versus Mach number components

Fig. 12 relates the new coefficient c_z to the M_x , M_z range of Fig. 11. The magnitude of the forces is directly indicated and the multiplication with the local dynamic pressure is no longer necessary.

UNSTEADY TWODIMENSIONAL FLOW

In contrast to other methods which use the steady data in tabular form as a numerical basis for unsteady calculations, the here presented steady model is a physical basis to evaluate unsteady aerodynamic coefficients. Because many authors wrote extensively about dynamic stall phenomena the present paper deals more with an easy general application.

PARAMETERS OF UNSTEADY AERODYNAMICS

Based on Mc Croskeys et. al. (Ref. 11) conclusions that the parameters of unsteady motion are more important than airfoil geometry, the earlier defined time dependent Mach number components M_x , M_z , dM_z/dx and the time derivatives \dot{M}_x , \dot{M}_z , $d\dot{M}_z/dx$ are the primary parameters of any arbitrary unsteady motion.

The airfoil shape influence considered in the steady model is extended to the unsteady case by similarity transformations.

For helicopter rotor application all motions can be expressed by a dominant first harmonic mode with the rotor rotational frequency and some higher harmonic modes. Now the reduced frequency in the form

$$k = \frac{\omega \cdot c}{a \cdot M_x \cdot 2} \quad (20)$$

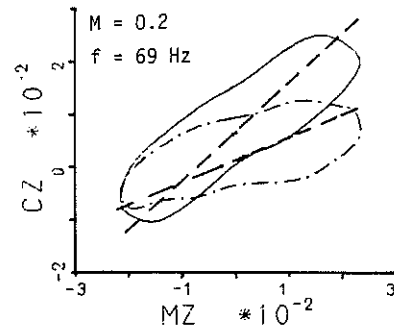
is introduced to describe this periodic behavior.

NONCIRCULATORY FLOW EFFECTS

The incompressible potential flow derivations for a flat plate by Greenberg (Ref. 12) can be easily expressed in the earlier defined coordinates because only velocity components perpendicular to the chord line are involved. Wayne Johnson (Ref. 13) payed attention to the problem of correct normal velocity identification at classical helicopter analyses. Here the general normal force coefficient is:

$$c_{z_{nc}} = \frac{c \cdot \pi}{2 \cdot a^2} \cdot \left(\dot{M}_z + \frac{d\dot{M}_z}{dx} \left(\frac{c}{4} - x_{AC} \right) \right) \quad (21)$$

This formula means physically the mass effect of an air cylinder with chord diameter idealised for a flat plate and therefore no corresponding effect in x direction.



NLR1 - TEST - NONC - STD

Fig. 13 Apparent mass effects

Fig. 13 shows the important effect of Eq. (21) on the shape of a 69 Hz pitch oscillation hysteresis (NLR1 Ref. 10) in attached flow. Exceptionally the steady reference line for the dashed - dotted curve is the fully separated flow term. It should be noted that Eq. (21) is incorrect at high accelerations. An approximate solution are the following functions:

$$\dot{M}_z = \dot{M}_z \cdot \frac{c_{nc}}{\dot{M}_z^2 + c_{nc}} \quad (22)$$

$$\frac{d\dot{M}_z}{dx} = \frac{d\dot{M}_z}{dx} \cdot \frac{c_{nc}}{(d\dot{M}_z/dx)^2 + c_{nc}} \quad (23)$$

The empirical coefficient c_{nc} accounts for compressibility effects in the accelerated flow and for a step function the forces are no longer infinite.

CIRCULATION LAG EFFECTS

Theoretical aerodynamic load prediction methods are available for arbitrary pitch and plunge motions or better for linear and constant velocity distributions perpendicular to the airfoil chord. In Ref. 14 the so called indicial functions of Wagner and Küssner are approximately represented by exponential functions. The assumption of harmonic motion and the use of Duhamel's integral (Ref. 14) leads to the following model consistent analytic formulation:

$$\Delta M_{z_w} = c \cdot M_x \cdot \sum_{i=1}^n \frac{2 \cdot a \cdot M_x \cdot \frac{dM_z}{dx}(t) \cdot \beta_{iw} + c \cdot \omega \cdot \frac{dM_z}{dx}(t - \frac{\pi}{2\omega})}{(c \cdot \omega)^2 + (2 \cdot a \cdot M_x)^2 \cdot \beta_{iw}^2} \cdot b_{iw} \quad (24)$$

in this case t means time

$$\Delta M_{z_k} = c \cdot \sum_{i=1}^n \frac{2 \cdot a \cdot M_x \cdot \dot{M}_z(t) \cdot \beta_{ik} + c \cdot \omega \cdot \dot{M}_z(t - \frac{\pi}{2\omega})}{(c \cdot \omega)^2 + (2 \cdot a \cdot M_x)^2 \cdot \beta_{ik}^2} \cdot b_{ik} \quad (25)$$

The coefficients β_{iw} , β_{ik} and b_{iw} , b_{ik} are those of Ref. 14 for Wagner and Küssner respectively. The unsteady component \dot{M}_z due to freestream is included in Eq. (25) and in contrast to Greenberg (ref. 12) where the reduced frequency is constant for freestream oscillations, the present method uses the local reduced frequency.

DYNAMIC STALL

As well reviewed by Ericsson and Reding (Ref. 15) dynamic stall is a viscous flow effect due to the unsteady motion induced boundary layer improvement or deterioration. The effect is similar to the earlier mentioned Reynolds number influence and causes a significant overshoot of lift. On the basis of the developed steady model dynamic stall is accounted for by the following separation point moving law:

$$\Delta M_{z_{ss}} = c_{os} \cdot M_x \cdot c \cdot \frac{2 \cdot a \cdot M_x \cdot \frac{dM_z}{dx}(t) \cdot c_{45} + c \cdot \omega \cdot \frac{dM_z}{dx}(t - \frac{\pi}{2\omega})}{(c \cdot \omega)^2 + (2 \cdot a \cdot M_x)^2 \cdot c_{45}^2} \quad (26)$$

The structure is similar to Eq. (24). c_{os} is the overshoot coefficient and c_{45} the reduced frequency where a phase angle of 45° is reached. The phase of overshoot is simply:

$$\psi = \arctg \left(\frac{k}{c_{45}} \right) \quad (27)$$

Fig. 14 gives a comparison of phase angles between the original Wagner function and the overshoot phase of Eq. (27). Ericsson (Ref. 16) made the so called leading edge jet effect responsible for the boundary layer difference between pitch and plunge. Following this assumption there exists a variation of Eq. (26) comparable to the variation from Eq. (24) to (25).

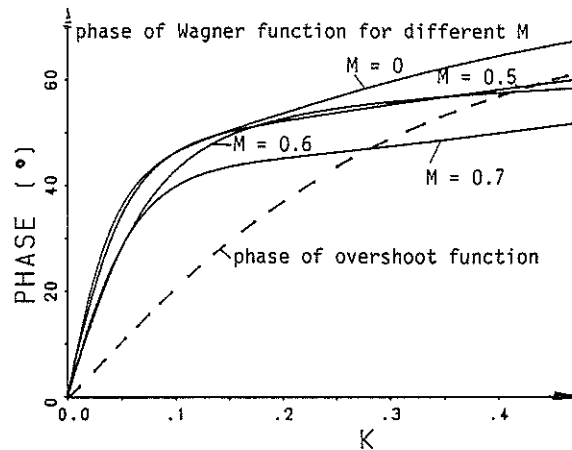


Fig. 14 Comparison of circulation lag and overshoot phase angles

VORTEX EFFECTS

At high frequencies, amplitudes and low Mach numbers a vortex forms on the leading edge, grows and travels to the trailing edge before leaving the airfoil. These spilled vortices give an additional increase in all aerodynamic coefficients. Implementation in the present method is possible with a separate vortex function similar to Eq. (10) using the phase laws developed by Ericsson and Reding (Ref. 17).

More attention is given to vortex proximity effects during fore and aft motion as measured by Maresca et al. (Ref. 18). Fig. 15 shows the significant effects of vortices even for combined motion. (Ref. 19)

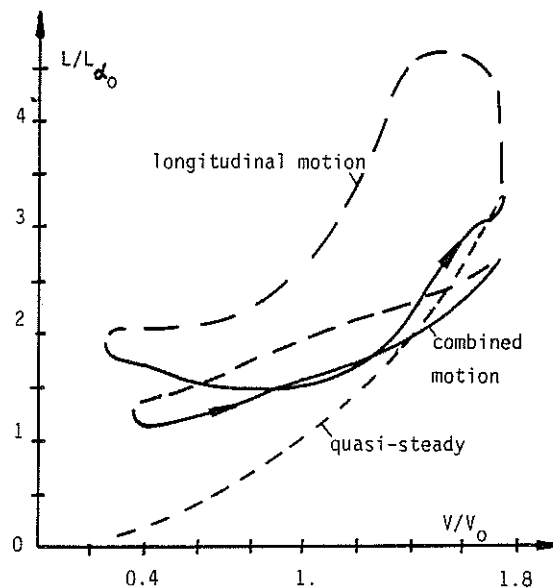


Fig. 15 Unsteady freestream effects on lift (Ref. 18, 19)

The circulation lag assumption for unsteady free-stream (Ref. 12) is not able to predict lift coefficients as high as 25. There must be a total lift lag due to vortex proximity when the airfoil is moving back in the own wake. The following expression was developed to predict approximately such significant effects:

$$\Delta M_x = c \cdot \frac{2 \cdot a \cdot M_x \cdot \dot{M}_x(t) \cdot \beta_{vp} + c \cdot \omega \cdot M_x(t - \frac{\pi}{2 \cdot \omega})}{(c \cdot \omega)^2 + (2 \cdot a \cdot M_x)^2 \cdot \beta_{vp}^2} \cdot b_{vp} \quad (28)$$

More measurements are necessary to prove this assumption. Because the local reduced frequency is used, the lag effects are highly nonlinear even for a harmonically varying freestream.

COMPARISON OF THE UNSTEADY SIMULATION MODEL WITH TEST DATA

The unsteady test data that were utilized for comparison are consequently those of Ref. 10. Here the full measured set of 340 hystereses is simulated by the present method based on the steady model. In a general simple version only the unsteady empirical overshoot parameter c_{os} was identified. The results of 159 hystereses at different reduced frequencies, mean angles of attack, amplitudes and Mach numbers are presented in the appendix. The correlation between theory and test is excellent except for the vortex effects at low Mach numbers which are not included in this simple version of analysis. The reason of presenting such a lot of hystereses loops is to demonstrate the overall correlation by the use of only one empirical parameter.

A comparison with the methods of Gormont (Ref. 20) and Gangwani (Ref. 2), who uses a lot of empirical parameters is illustrated by Fig. 16. Additional data of Gray and Liiva (Ref. 21) are used.

The unsteady deviation of the present model from test is about twice that of the steady basis and lies within the measurement inaccuracies.

Now a method is at hand to simulate steady and unsteady twodimensional aerodynamic coefficients on the basis of a relatively simple representation of viscous and inviscid flow effects and by use of fundamental theoretical results.

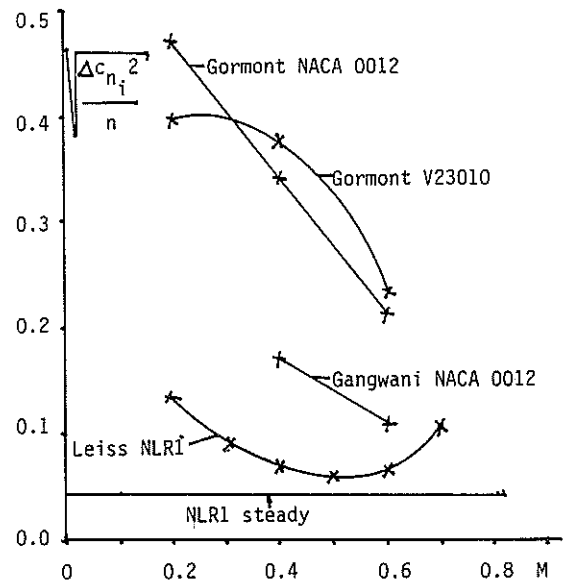


Fig. 16 Comparison of the present method with other models

CONCLUSIONS

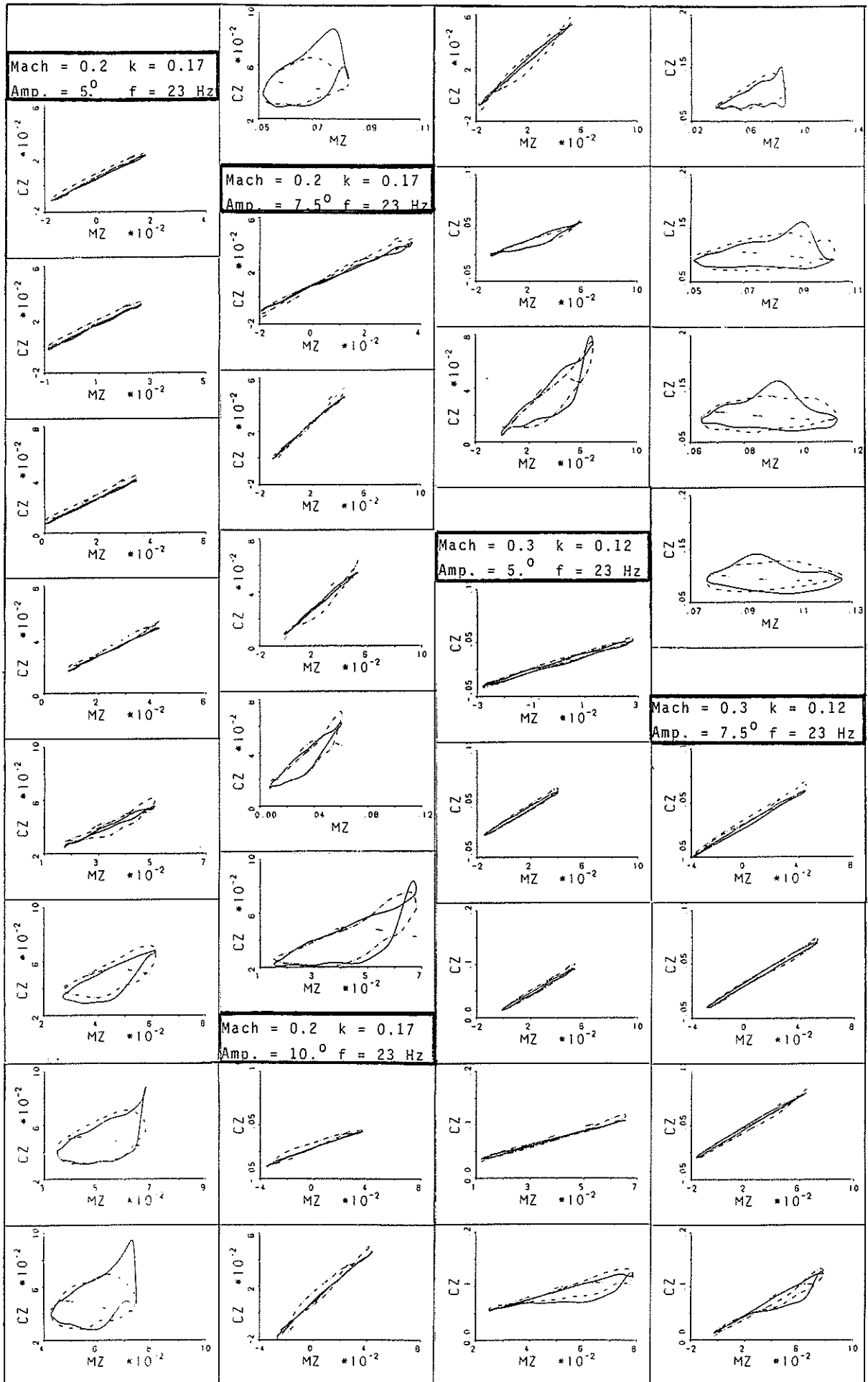
- o A general formulation has been developed to simulate steady and on this basis unsteady aerodynamic coefficients.
- o Important flow phenomenas were implemented on one side by existing theoretical calculations and on the other side by empirical parameters.
- o New definitions, expressed in Mach number components were formulated to couple directly blade aerodynamics with external flow components and with the mechanical derivation of mass forces.
- o The influence of compressibility, Reynolds number and different types of steady stall was considered.
- o Different flow type functions made it possible to simulate continuously attached flow, partially stalled flow and fully separated flow for all angles of attack including reverse flow.
- o All three types of unsteady motion, pitch, plunge and fore and aft motion have primary influence on the unsteady aerodynamic coefficients.
- o The parameters of unsteady motion and their time derivatives are more important than the airfoil shape which is considered by similarity transformations.

- o An excellent correlation between test data and the present simulation model is demonstrated with only one empirical unsteady parameter.
- o Correlation is within the measurement accuracy and the comparison with other methods indicates a significant progress.
- o analytical integration is possible in radial direction through the special form of flow functions.
- o The method must be extended to threedimensional flow effects especially sweep and blade tip relief for future.

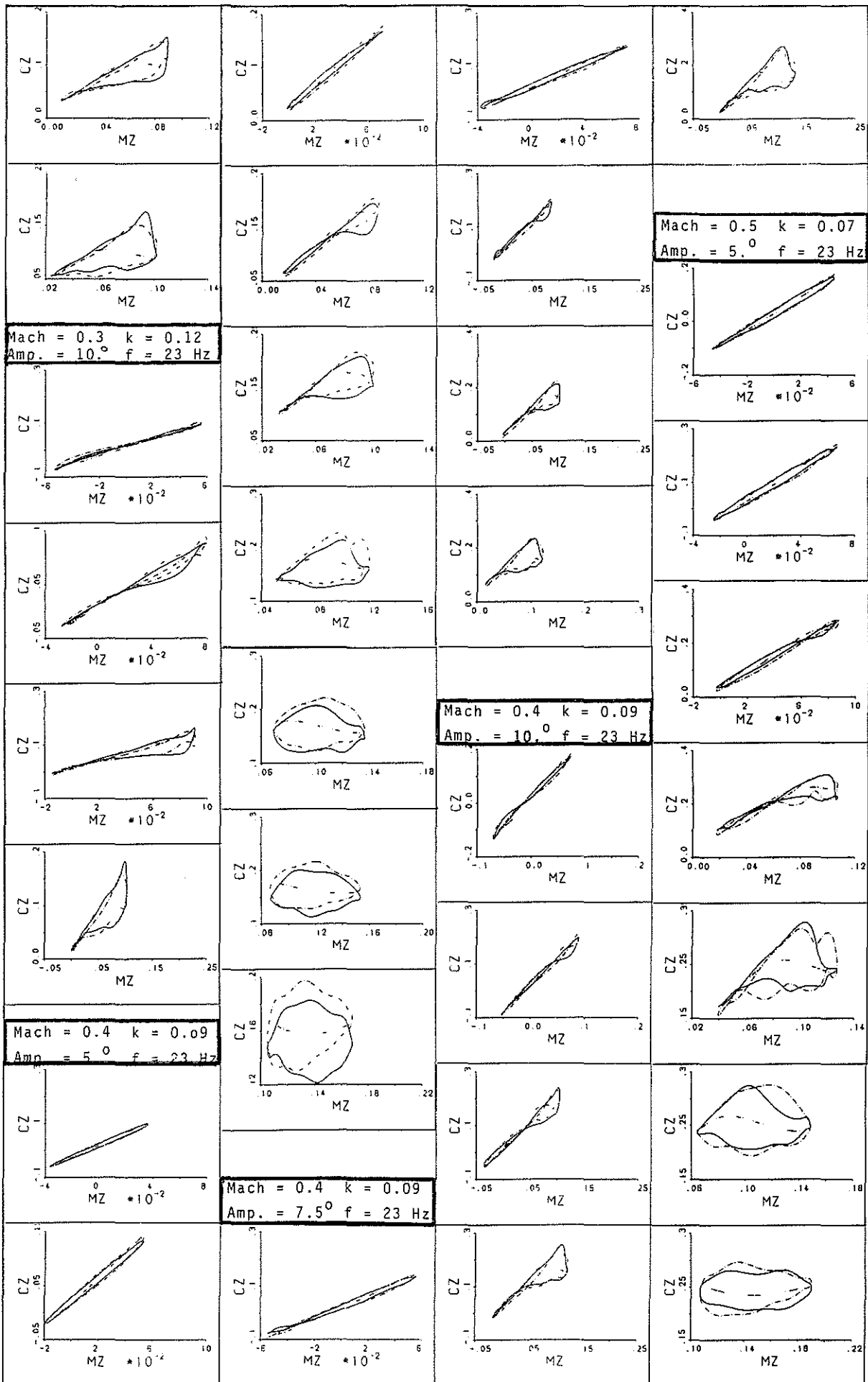
REFERENCES

- 1) Beddoes, T.S., Practical computation of unsteady lift, Paper presented at the 8 th European Rotorcraft Forum, Aix en Provence, 1982
- 2) Gangwani, S.T., Synthesized airfoil data method for prediction of dynamic stall and unsteady airloads, Paper presented at the 39 th Annual Forum of the American Helicopter Society, St. Louis, 1983
- 3) Petot, D., Progress in the semi-empirical prediction of the aerodynamic forces due to large amplitude oscillations of an airfoil in attached or separated flow, Paper presented at the 9 th European Rotorcraft Forum, Stresa, 1983
- 4) Theodorsen, T., General theory of aerodynamic instability and the mechanism of flutter, NACA Report 496, Va., 1934
- 5) Hoerner, S.F., Fluid dynamic drag, published by the author, 1965
- 6) Critzos, C.C. et. al., Aerodynamic characteristics of NACA 0012 airfoil section at angles of attack from 0° to 180° , NACA TN 3361, Va., 1954
- 7) Dadone, L.U., US Army helicopter design DATCOM, Volume 1 - Airfoils, USAAMRD CR 76-2, 1976
- 8) Yamauchi, G.K., Johnson, W., Trends of Reynolds number effects on two-dimensional airfoil characteristics for helicopter analyses, NASA TM 84363, April, 1983
- 9) USAF Stability and Control DATCOM, McDonnell Douglas Aircraft Corporation, Air Force Flight Dynamics Laboratory, Wright-Patterson Air Force Base, Ohio, February, 1972
- 10) Dadone, L.U., Two-dimensional wind tunnel test of an oscillating rotor airfoil, Volume II, NASA CR 2915, Philadelphia, 1977
- 11) McCroskey, W.J. et. al., Dynamic stall on advanced airfoil sections, Journal of the American Helicopter Society, Vol. 26, No. 3, July, 1981
- 12) Greenberg, J.M., Airfoil in sinusoidal motion in a pulsating stream, NACA TN 1326, Langley Field, September, 1946
- 13) Johnson, W., Application of unsteady airfoil theory to rotary wings, Journal of Aircraft, Vol. 17, No. 4, April, 1980
- 14) Bisplinghoff, R.L. et. al., Aeroelasticity, Addison-Wesley Publishing Co., Reding, Mass., 1955
- 15) Ericsson, L.E., Reding, J.P., Dynamic stall analysis in light of recent numerical and experimental results, Journal of Aircraft, Vol. 13, No. 4, April, 1976
- 16) Ericsson, L.E., Reding, J.P., The difference between the effects of pitch and plunge on dynamic airfoil stall, Paper presented at the 9 th European Rotorcraft Forum, Stresa, 1983
- 17) Ericsson, L.E., Reding, J.P., Dynamic stall at high frequency and large amplitude, Journal of Aircraft, Vol. 17, No. 3, March, 1980
- 18) Maresca, C. et. al., Experiments on an airfoil at high angle of incidence in longitudinal oscillations, Journal of Fluid Mechanics, Vol. 92, part 4, 1979
- 19) Maresca, C., Unsteady aerodynamics of an Airfoil at high angle of incidence performing various linear oscillations in a uniform stream, Paper presented at the 5 th European Rotorcraft Forum, Amsterdam, September, 1979
- 20) Gormont, R.E., A mathematical model of unsteady aerodynamics and radial flow for application to helicopter rotors, USAAMRD Technical Report 72-67, 1972
- 21) Gray, L., Liiva, J., Two-dimensional tests of airfoils oscillating near stall, Vol. II, Data Report, USAAVLABS Technical Report 68-13B, 1968

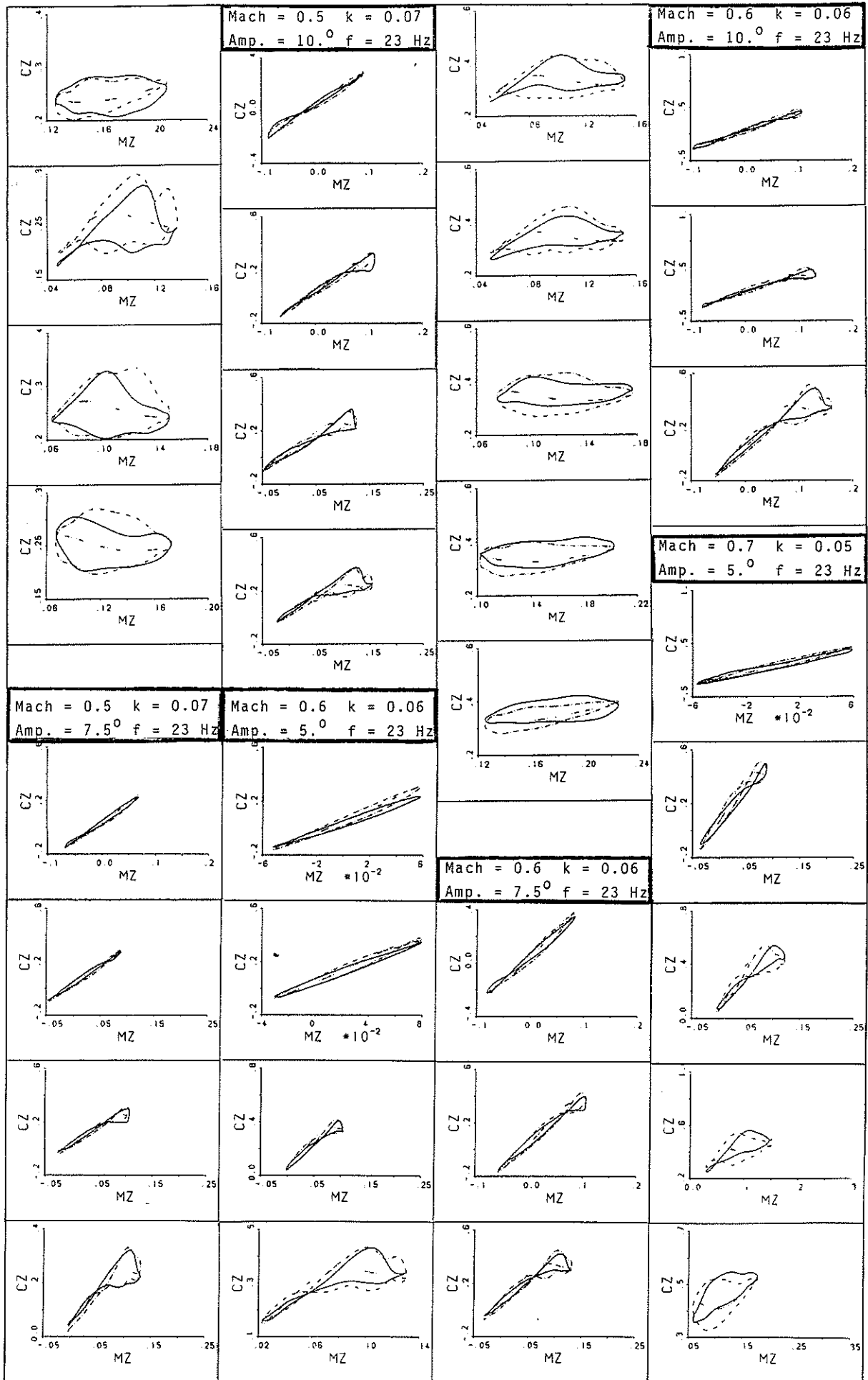
COMPARISON OF UNSTEADY NLRI MEASUREMENTS WITH THEORY: —TEST --.MODEL ---.STEADY



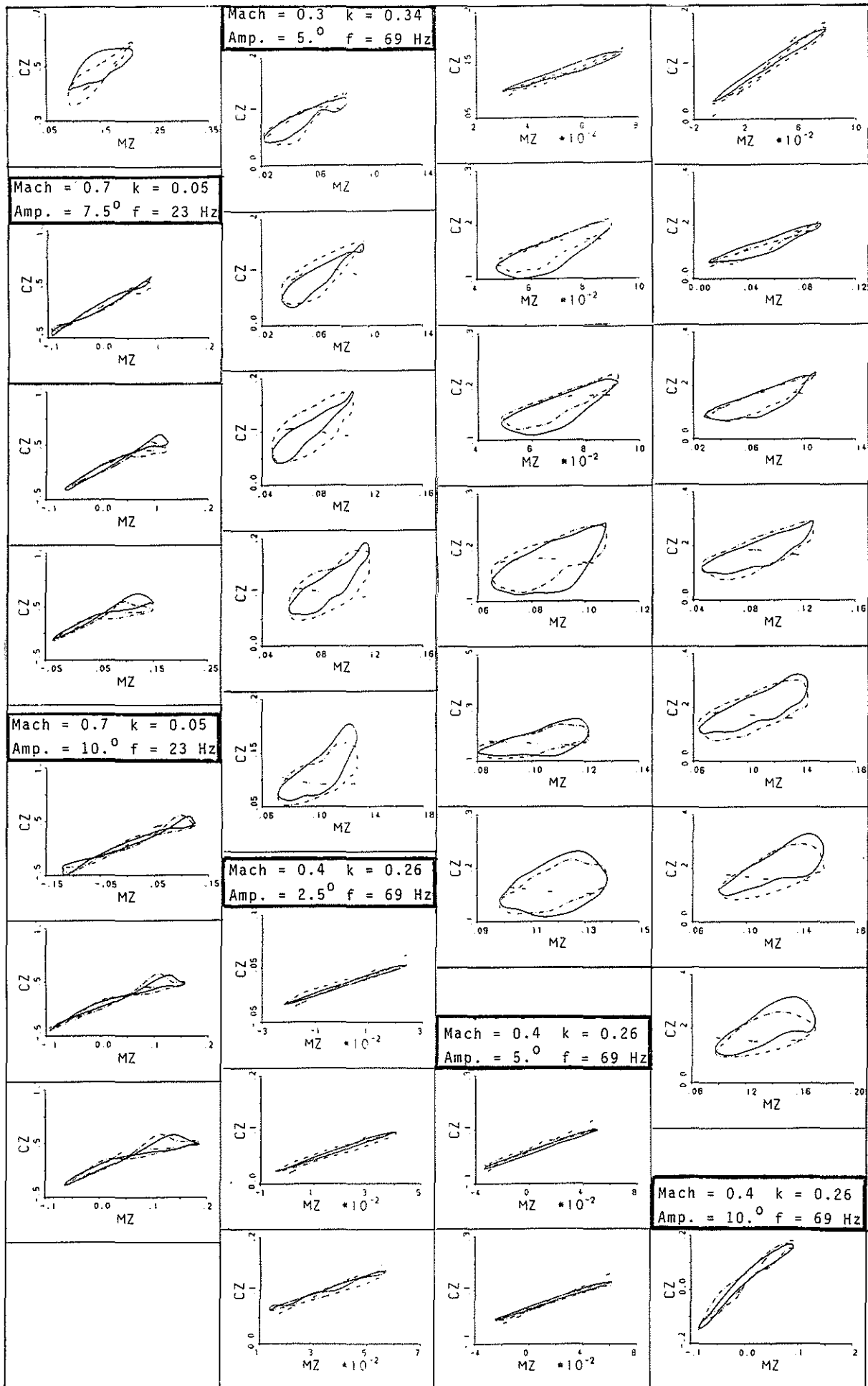
COMPARISON OF UNSTEADY NLR1 MEASUREMENTS WITH THEORY: —TEST --.MODEL ---.STEADY



COMPARISON OF UNSTEADY NLR1 MEASUREMENTS WITH THEORY: --TEST --.MODEL ---.STEADY



COMPARISON OF UNSTEADY NLRI MEASUREMENTS WITH THEORY: —TEST --.MODEL ---.STEADY



COMPARISON OF UNSTEADY NLRI MEASUREMENTS WITH THEORY: —TEST - .MODEL ---.STEADY

